Journal of Physics: Conference Series

PAPER • **OPEN ACCESS**

Benchmarking different fidelities in wind turbine aerodynamics under yaw

To cite this article: A Muñoz-Simón *et al* 2020 *J. Phys.: Conf. Ser.* **1618** 042017

View the article online for updates and enhancements.



IOP ebooks™

Bringing together innovative digital publishing with leading authors from the global scientific community.

Start exploring the collection–download the first chapter of every title for free.

This content was downloaded from IP address 155.198.10.231 on 10/05/2021 at 15:17

Benchmarking different fidelities in wind turbine aerodynamics under yaw

A Muñoz-Simón[1], R Palacios[2], A Wynn[3]

[1] Early Stage Researcher, *Imperial College London*, *Department of aeronautics*, South Kensington Campus, London SW7 2AZ, UK
[2] Professor, *Imperial College London*, *Department of aeronautics*, South Kensington Campus, London SW7 2AZ, UK
[3] Senior lecturer, *Imperial College London*, *Department of aeronautics*, South Kensington Campus, London SW7 2AZ, UK

E-mail: a.munoz-simon@imperial.ac.uk

Abstract. This paper analyses the aerodynamics of wind turbines under yaw with different modelling fidelities (BEM, BEM with skewed wake model, UVLM and LES-AL). First of all, models are compared in a zero-yaw case to demonstrate their accuracy in prediction of out-of-plane loads and the discrepancy of UVLM in the in-plane loads due to the lack of viscous drag. Secondly, the yaw aerodynamics are described through the *advancing/retreating* and *skewed wake* effects, which are appropriately captured by UVLM and LES-AL and lead to an incorrect prediction of the location of maximum and minimum loading along a revolution by BEM. Further, when a skew-wake model is included in BEM, it predicts the correct locations but exhibits overly large loading variations. These predictions are consistent for all yaw angles studied ($\gamma = 10^\circ - 30^\circ$). All solvers predict similar decrease of root-bending moments, rotor power and thrust coefficients up to a yaw angle of 10°. However, at larger yaw angles, BEM overpredicts this decrease of coefficients with the yaw angle due to the unsuccessful performance of yaw corrections as opposed to UVLM that inherently accounts for three-dimensional effects. This study demonstrates the need to use computational models that can account for three-dimensional effects in the computation of aerodynamic loads for yaw angles above 10°.

1. Introduction

Wind turbines can operate under yawed conditions due to errors in the alignment mechanism or due to its long reaction time that cannot accommodate rapid changes in wind direction [1]. In these conditions, the yaw angle is relatively small, typically below 10°. Nevertheless, the possibility of voluntarily operating wind turbines under yaw is very valuable because it allows steering the turbine wakes such that the negative influence on the downstream wind turbines are reduced [2]. In this situation, the first wind turbine rotor is not perpendicular to the wind reducing its power production. However, the downstream wind turbines are not so negatively influenced by the upstream wind turbine and thus generate more power. If the wind farm is optimised as a whole, this philosophy can give rise to increased power production of the wind farm. In these cases, yaw angles of up to 30° may be required.

The computation of loads and power under yaw is important because the associated fluctuating loads generate significant fatigue [3]. Moreover, this computation is challenging because it involves aerodynamic effects that are computationally expensive and difficult to model


Content from this work may be used under the terms of the Creative Commons Attribution 3.0 licence. Any further distribution of this work must maintain attribution to the author(s) and the title of the work, journal citation and DOI.
Published under licence by IOP Publishing Ltd

[4]. These effects are characterised by unsteadiness and three-dimensional flow arising from the varying wind incidence along a revolution and the interaction between blade sections.

There are different computational fidelities to estimate aerodynamic loads [5]. For example, Blade Element Momentum theory is based on steady assumptions and gives rise to very efficient codes. However, BEM must be corrected to account for complex aerodynamic effects. Unsteady Vortex Lattice Method provides a compromise between accuracy and efficiency assuming inviscid flow but capturing unsteady and three-dimensional effects. Finally, Large Eddy Simulation coupled with Actuator Line theory is an expensive option which allows the study of interactions between wind turbines and wakes through the simulation of the whole velocity field. There are other fidelities not analysed in this paper, which are both accurate and expensive, such as blade-resolved Unsteady Reynolds-Averaged Navier Stokes.

This paper studies the loads under yaw at different levels of detail (local loads at several spanwise positions, root-bending moments and rotor coefficients) for the three modelling fidelities described in Section 2. In Section 3.1, the case of zero yaw is established as baseline for the comparison. Afterwards, the physical phenomena appearing in yaw cases and the ability of different solvers to capture it are described in Section 3.2 for the case of 30° yaw. Finally, the limitations of each fidelity are defined as a function of the yaw angle in Section 3.3.

2. Methodology

A description of the basic theory behind each modelling fidelity is included because it affects the physical phenomena that each method is able to capture. The theories employed in this work are well known, so only a brief overview associated with the yaw computations is provided. Finally, the wind turbine model selected for the analysis and the computational details are included.

2.1. Blade Element Momentum

The main advantage of Blade Element Momentum (BEM) methods is their efficiency which is achieved through the connection of two theories suitable for steady cases [6]. The first is the momentum theory that relates global flow velocities and the pressure drop across the wind turbine with the forces generated on solid surfaces. The second theory defines the aerodynamic forces in each radial section of the blade based on the local velocity and previously-identified two-dimensional aerodynamic data usually obtained from wind tunnel measurements or computational methods. However, important three-dimensional effects are not modelled which require BEM to use semi-empirical corrections [7] for rotation, tip and root ends and wake deviation effects. These corrections are usually tailored to the more simple cases, leading to errors in more complex ones [8], such as unsteady inflow or large yaw angles.

OpenFAST is the open-source [9] version of FAST (Fatigue, Aerodynamics, Structures and Turbulence) which is the aeroelastic code for horizontal-axis wind turbines of the National Renewable Energy Laboratory (NREL). In the present work, it is used under two settings. First, a basic BEM configuration (*WakeMod=1*) is employed without a skewed wake model. Second, a dynamic BEM model (*WakeMod=2*) is used with the Pitt and Peters model for skewed wake. These are referred as *"BEM no skew"* and *"BEM skew"*, respectively. In the *BEM skew* case, very small differences have been found between *WakeMod* 1 and 2, indicating that the skew wake model is the main driver of the differences. In both cases, unsteady airfoil aerodynamics are accounted for by Gonzalez's variation of Beddoes-Leishman theory [10].

2.2. Unsteady Vortex Lattice Method

Unsteady Vortex Lattice Method (UVLM) [11] aims to capture unsteady and three-dimensional aerodynamic effects at an intermediate computational cost through the assumption of inviscid flow. This neglects viscous effects and consequently these methods cannot capture phenomena such as flow separation or viscous drag. Moreover, other simplifications are usually assumed to

improve computational efficiency, e.g., solid bodies are reduced to flat surfaces, neglecting the effect of thickness. Vortex methods have already been used in wind energy [12, 13].

SHARPy stands for Simulation of High Aspect Ratio Planes in Python [14] and is an aeroelastic code partially developed by the authors [15]. It uses the UVLM for its aerodynamic model [16]. Specifically, the singularity of the velocity field is solved using a core of 10^{-6} m.

2.3. Large Eddy Simulation - Actuator Line

Large Eddy Simulation - Actuator Line (LES-AL) models were conceived to capture the interactions between wind turbines and wakes within a wind farm and the effect of atmospheric flows. This requires accounting for a very wide range of scales which are split between two models and subsequently coupled together. Wind turbine aerodynamics can be simulated through the AL technique [17] which samples the flow field velocity and applies certain corrections (similar to BEM methods) to compute the effective angle of attack at blade positions. This information is then used to retrieve the force generated on the blade using 2D airfoil data from look up tables. LES uses 3D domain discretisation methods to resolve the large scales of the flow field and parametrises small-scale turbulence [18]. The influence of the wind turbines is accounted for through the extraction of momentum from the flow at the blade positions based on the previously-described force estimation. This method is considered of high-fidelity according to the wake-to-turbine interactions but uses a simplified estimation of the aerodynamic forces.

WInc3D is a wind farm simulator developed by a team at Imperial College London to study the flow structure and turbulence in wind farms [19]. It uses finite differences, an in-house AL model and, in this case, a constant Smagorinsky explicit LES model.

2.4. Simulation set up

The AVATAR wind turbine is a benchmark case for large offshore wind turbines [20]. Its main characteristics are: 10 MW of nominal power, 102.88 m rotor radius and 137.5 m hub height. In this case no tilt, prebending or presweep are applied [21]. The operation point has been chosen at the end of the optimal production region of the power curve, namely an incoming wind speed of 10.5 m/s, a rotation velocity of 0.945 rad/s (tip-speed ratio equal to 9.26) and zero pitch.

The OpenFAST discretisation includes 51 nodes. The simulations have a time step of 0.5° and were run for 5 revolutions. In SHARPy simulations, blades are discretised with 14 elements (three nodes each) in the spanwise direction. The aerodynamic surface is composed of 64 panels in the chordwise direction. A time step equivalent to 2° was employed for seven revolutions. Moreover, the wake length used is equivalent to seven rotor revolutions and it convects downstream based on the external velocity and accounting for self-induction, which is found to be essential to capture blade loads (around 4% and 8% difference in C_T and C_P respectively). WInc3D uses 105 nodes to discretise the blade. Moreover, the fluid domain covers 5 rotor diameters in the wind direction and 4 diameters in the other two with 2 m cells. The wind turbine is placed two rotor diameters downstream from the computational inflow. The simulations have a time step of 0.5° and were run for 12 revolutions.

3. Results

Section 2 describes fundamental differences among the selected modelling fidelities. Section 3.1 aims to establish a benchmark example for models comparison using the case of zero yaw ($\gamma = 0°$) in which only very basic aerodynamic phenomena play a role. Afterwards, Section 3.2 analyses the aerodynamic effects induced by non-zero yaw and how they are captured by different theories in the extreme case of $\gamma = 30°$. Finally, Section 3.3 describes the strength of these effects for milder yaw angles with the objective of defining the range of validity for each fidelity.

3.1. Reference case for rotor aerodynamics ($\gamma = 0°$)

In the case of zero-yaw, inflow to the wind turbine is uniform and perpendicular to the rotor plane, the wind incidence on the blade does not change with the azimuthal position (θ) and this generates constant loading along a revolution. This case is appropriate for a comparison of fidelities because it shows the very basic characteristics of each model in a situation with no complex aerodynamic phenomena. BEM methods have been adjusted for these cases in the past and thus are very accurate.

Figure 1 shows the out-of-plane ($C_{\text{out}}/d(r/R)$) and in-plane ($C_{\text{in}}/d(r/R)$) force coefficients per unit non-dimensional span ($d(r/R)$) for the four fidelities. The out-of-plane coefficient is mainly determined by the lift of the aerodynamic section and is very well captured by all the codes. In the case of the in-plane coefficient, both in-plane projections of the lift and drag forces are comparable and thus significant. The in-plane projection of lift points on the same direction of the blade velocity which generates positive in-plane coefficient and power. However, the in-plane projection of drag points on the opposite direction which generates negative in-plane coefficient and thus reduces the power production. BEM and LES-AL models include drag as tabulated airfoil data and thus their agreement is very good. However, UVLM predicts a larger in-plane coefficient because it does not account for the friction drag losses. This effect is specially noticeable near the root because in this region UVLM panels generate lift despite being a very thick cross-section. UVLM and LES-AL account inherently for tip effects, however, BEM methods require the application of corrections. There is a very good agreement between UVLM and BEM methods and a small discrepancy of LES-AL method associated with the grid size (which may be too coarse in that region).

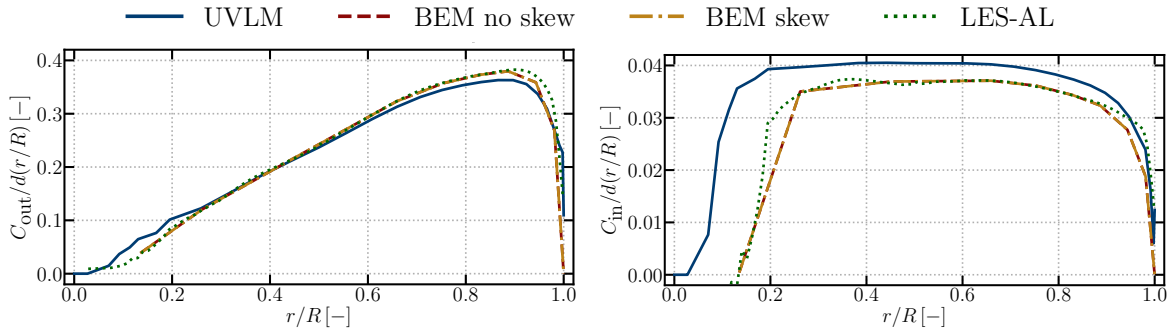


Figure 1: Spanwise loads ($\gamma = 0°$)

In the rest of this report, the left-hand side subplot of each figure shows variables associated with the out-of-plane forces, which are predominantly responsible for wind turbine loading. The right-hand side subplots show in-plane loads responsible for power generation and are less critical from a structural analysis viewpoint. The differences in the steady-state values of Fig. 1 appear consistently in the subsequent analysis.

3.2. Rotor aerodynamics in extreme yaw ($\gamma = 30°$)

The extreme case of $\gamma = 30°$ (according to FAST sign convention) has been chosen next to make the effects obvious. In yaw cases, the loads along a revolution are not constant and, thus, time series are shown below. However, Figure 2 shows the average of these loads along a revolution which reveals a decrease of both coefficients with respect to the zero-yaw case (Fig. 1).

The variation of the loads along a revolution in yaw cases (as opposed to the $\gamma = 0°$ case) can be explained through the interaction between two effects [22]: the *advancing/retreating* effect and the *skewed wake* effect. To simulate these effects, models should account, in principle, for

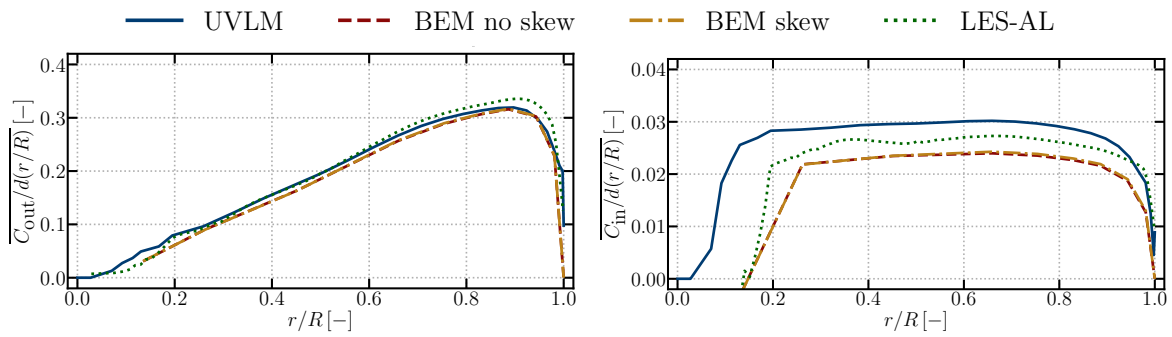


Figure 2: Average spanwise loads ($\gamma = 30°$)

unsteady and three dimensional aerodynamics. Regarding unsteadiness, yaw inflow is steady itself but has an unsteadiness associated to blade rotation because the relative orientation between the inflow and the blade changes along a revolution. In this case the reduced frequencies for the airfoils at $r/R = 0.45$ and $r/R = 0.75$ are 0.055 and 0.022, respectively. Thereby, yaw loads can be reasonably approximated by a quasi-steady assumption. Regarding three dimensional effects (tip and root ends, azimuthal variations of induction and interaction between radial sections), only UVLM can inherently account for them according to section 2. The best way to show the *advancing/retreating* and the *skewed wake* effects is by looking at different spanwise positions on the blade analysing how loads change along a revolution. This is done for two radial positions ($r/R = 0.45$ and $r/R = 0.75$) in Figures 3 and 4, respectively.

The *advancing/retreating* effect accounts for the change in angle of attack along a revolution due to the change in relative orientation between the blade and the incoming wind. For example, at the top position (for positive yaw angles) the blade rotation is in the same direction as the in-plane component of the incoming wind which increases the angle of attack with respect to the reference case. This effect generates maximum and minimum loading at $\theta = 0°$ and $\theta = 180°$. This effect is less noticeable near the tip, since the velocity of the blade due to rotation is dominant there. Figure 3 shows the out-of-plane and in-plane force coefficients at $r/R = 0.45$. UVLM, BEM *no skew* and LES-AL predict coherent locations of maxima and minima according to the previous theory for the in-plane coefficient but not in the out-of-plane coefficient whose variations are, nonetheless, very small. These quasi-steady effects should be captured by all the solvers, however, BEM *skew* do not predict the correct position of the maximum and minimum loading because the influence of the *skewed wake* effect is highly overestimated and goes beyond its real influence region.

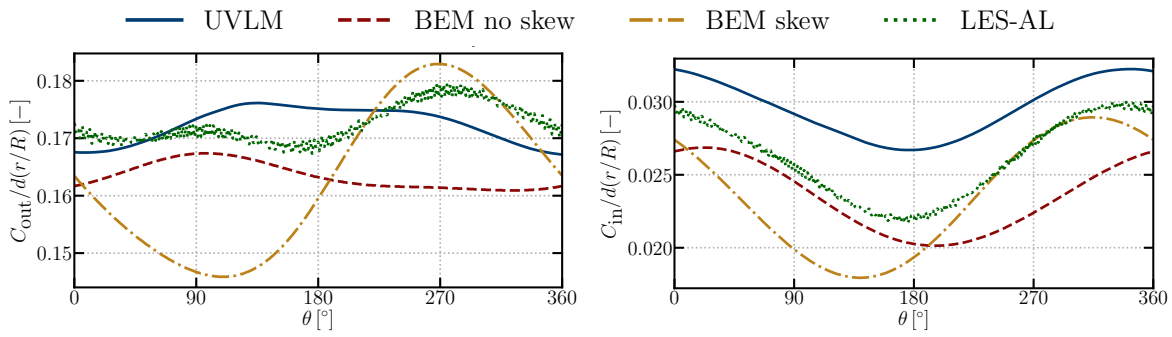


Figure 3: Azimuthal variations of loads at $r/R = 0.45$ ($\gamma = 30°$)

The *skewed wake* effect accounts for the non-axisymmetric velocity deficit behind a wind turbine in yaw. As a consequence, blades travel through regions of varying velocity deficit which generates oscillating induction along a revolution. These oscillations are stronger near the tips and thus this effect is more important in the outer part of the blade. In particular, blades are near the strongest velocity deficit region when they are in the downwind position ($\theta = 90°$) where they undergo large induction and thus the loading reaches a minimum. At $\theta = 270°$ the blade is close to the mildest velocity deficit region where induction is at a minimum and loads at a maximum. Figure 4 shows the prediction of the load coefficients at $r/R = 0.75$. It shows that the corrections applied to the BEM *skew* model are useful to reproduce the location of the maxima and minima according to the previous explanation of the *skewed wake* effect. However, they lead to larger variations of the loads compared to UVLM and LES-AL that can inherently account for this effect. Moreover, BEM *no skew* lacks a wake model to capture the induction change along a revolution and thus it predicts wrong locations of maximum and minimum loading.

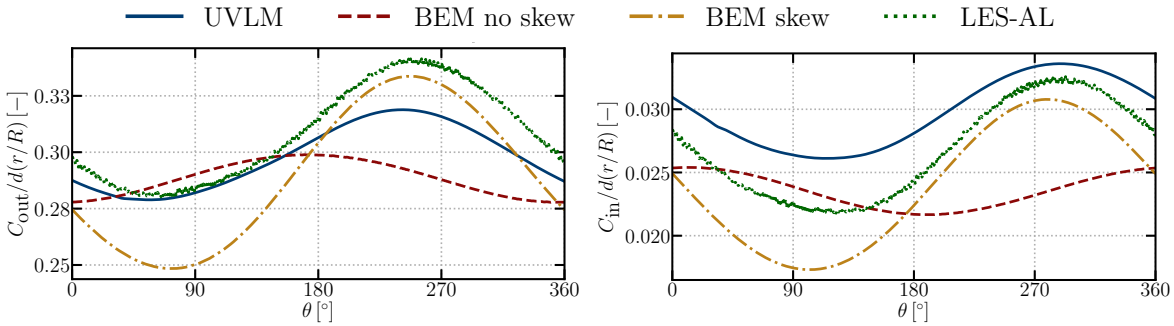


Figure 4: Azimuthal variations of loads at $r/R = 0.75$ ($\gamma = 30°$)

Figures 3 and 4 have shown local aerodynamic force coefficients to investigate yaw aerodynamics in detail. However, in load analysis it is more common to use the integration of these coefficients along the blade, namely the root-bending moments (M_{out} and M_{in}). In this integration, the tip region is the most important contributor and thus, the location of maximum and minimum root-bending moments along a revolution (Fig. 5) follows the same pattern as the force coefficients in the tip region (Fig. 4). Specifically, the minimum and maximum root-bending moments should appear at positions close to $\theta = 90°$ and $\theta = 270°$, respectively. Figure 5 shows that UVLM, BEM *skew* and LES-AL methods are able to capture these positions, however, the variations predicted by the BEM *skew* model are very large. Finally, BEM *no skew* provides the wrong positions.

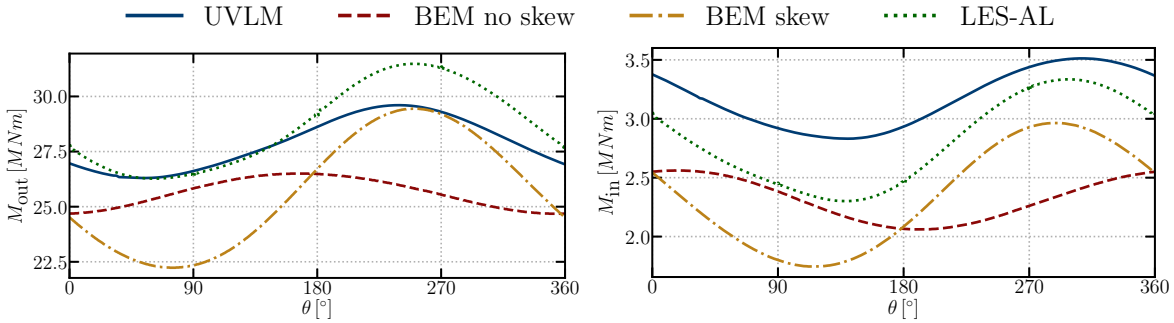


Figure 5: Azimuthal variations of root-bending moments ($\gamma = 30°$)

Finally, the rotor integrated coefficients of thrust (C_T) and power (C_P) provide a simple metric to define the rotor operating state (Figure 6). The maximum difference in thrust coefficient between solvers has turn from 2% in the case of $\gamma = 0°$ to 8% in the case of $\gamma = 30°$ due to the differences in the yaw aerodynamic modelling explained in this section. Moreover, in the case of $\gamma = 0°$ UVLM already predicted 13% higher C_P than the other solvers due to the absence of friction drag. In the case of $\gamma = 30°$ yaw, UVLM predicts even higher C_P than both BEM and LES-AL (30% and 12% respectively) due to the different modelling accuracy of yaw aerodynamics which is further investigated in section 3.3. Finally, Figure 6 shows that the large fluctuations along a revolution of local load coefficients showed in Figures 3 and 4 have almost disappear in the case of rotor coefficients due to the balancing effect between the three blades.

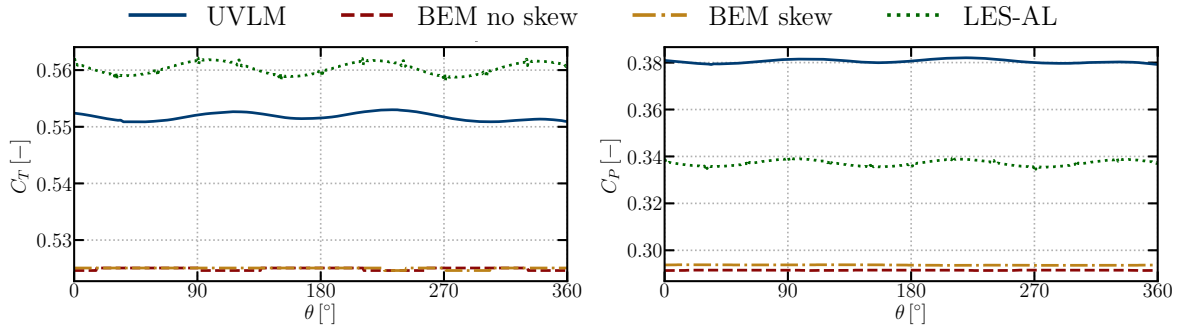


Figure 6: Azimuthal variations of rotor thrust and power coefficients ($\gamma = 30°$)

This section has shown that to capture the local behaviour of loads under yaw, the computational method used needs to account for three dimensional effects, as UVLM and LES-AL do. This behaviour is noticeable at the level of root-bending moments, but not when rotor integral quantities are considered.

3.3. Rotor aerodynamics as a function of the yaw angle ($0° \leq \gamma \leq 30°$)
In the previous section, the effect on loads of the extreme case of 30° yaw was analysed. This section aims to analyse the effect of milder yaw angles. To reduce the amount of data presented, this will be achieved via analysis of several statistics: the average ($\overline{\bullet}$) and standard deviation ($\sigma(\bullet)$) of fluctuations and the position of maximum and minimum loading along a revolution ($\theta(\bullet)_{\max}$ and $\theta(\bullet)_{\min}$). As in the previous section, loads at two spanwise positions ($r/R = 0.45$ and $r/R = 0.75$), root-bending moments and rotor coefficients are studied.

Figures 7 and 8 show the statistics for the in-plane and out-of-plane coefficients at $r/R = 0.45$ and $r/R = 0.75$ respectively. All solvers predict very small changes in the position of maxima and minima of both coefficients with the yaw angle. Thus, the differences for these variables explained in section 3.2 ($\gamma = 30°$), apply to the whole studied range of yaw angles. Moreover, the reduction in average loading is similar for all the codes for the smallest yaw angles ($\gamma \leq 10°$) implying that the differences between solvers explained for the $\gamma = 0°$ case are valid for small yaw angles. However, when the yaw angle increases further ($\gamma \geq 20°$) the performance degradation predicted by BEM methods is significantly larger. UVLM and LES-AL are the most adequate methods to capture three-dimensional effects, which are the main sources of fluctuations along a revolution. In general, BEM *no skew* predicts too small fluctuations and BEM *skew* too large. Moreover, UVLM and LES-AL fluctuations are closer but LES-AL ones are still larger.

Figure 9 shows the same statistics for the root-bending moments. Again, the location of the maxima and minima does not change significantly with the yaw angle. As explained before, the value of the loads at $\gamma = 0°$ for UVLM is not as accurate as for the rest of the methods. However,

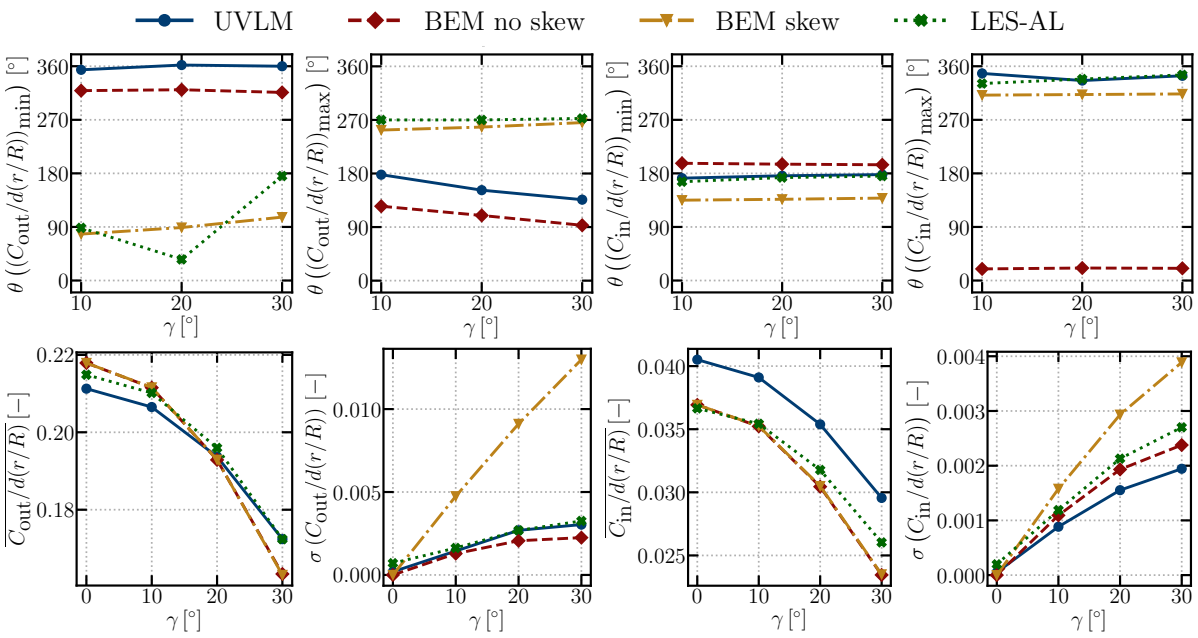


Figure 7: Yaw effect on loads at $r/R = 0.45$

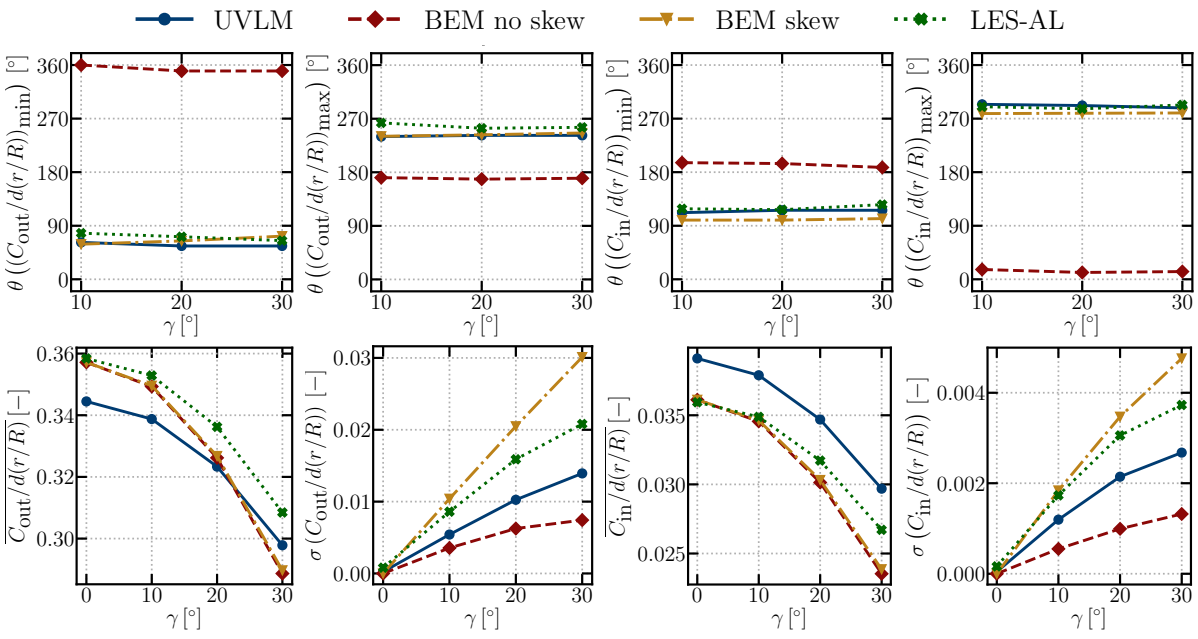


Figure 8: Yaw effect on loads at $r/R = 0.75$

the reduction in average load and the increase in standard deviation come from physical effects that only UVLM and LES-AL can properly capture. On that basis, BEM methods predict coherent average decrease up to $\gamma = 10°$ but excessive decrease after this point. UVLM and LES-AL estimate similar decay. Again, BEM *skew* predicts too large fluctuations and BEM *no skew* too small.

Finally, Figure 10 shows the effect of yaw on rotor coefficient. It is important to point out that these coefficients imply an important averaging effect and, consequently, their standard

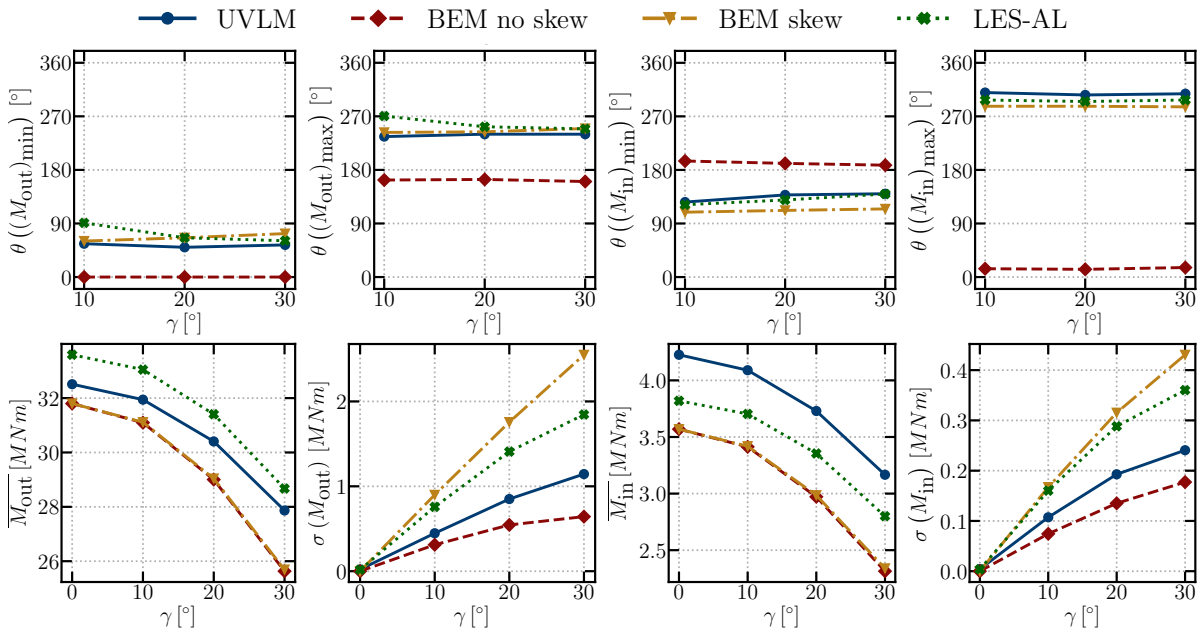


Figure 9: Yaw effect on root-bending moments

deviation is very small. It is small enough to evidence the numerical noise in UVLM and LES-AL in the case of $\gamma = 0°$ which should be exactly zero. It is interesting that, albeit small, UVLM and LES-AL predict larger fluctuations along a revolution. All the models agree on predicting a significant increase of the fluctuations for very high yaw angles ($\gamma \geq 20°$).

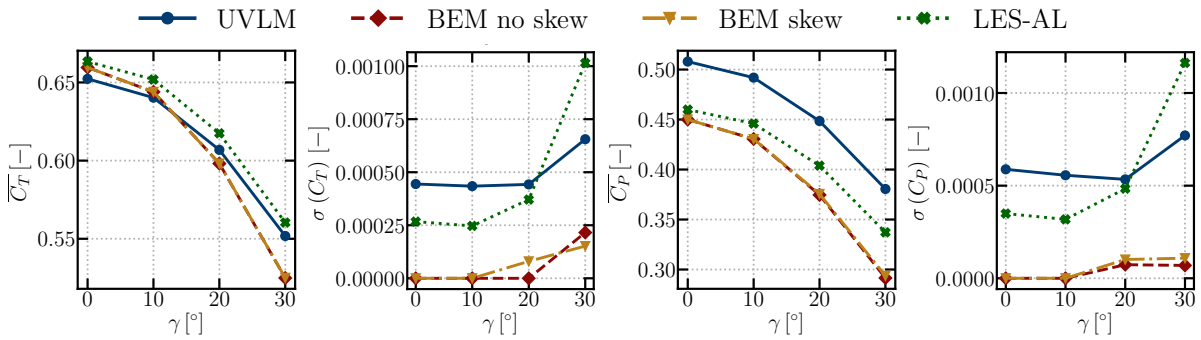


Figure 10: Yaw effect on rotor coefficients

4. Conclusions

The aerodynamics of wind turbines under yaw is a complex phenomenon that requires physics-based models to be adequately simulated. This paper has analysed the accuracy of different modelling fidelities (BEM *no skew*, BEM *skew*, UVLM and LES-AL) in this scenario.

BEM methods have been adjusted for several decades to match the behaviour of wind turbines in the case of uniform flow perpendicular to the rotor plane (zero yaw, $\gamma = 0°$). On the one hand, this scenario has shown good estimation of loads by LES-AL when compared to BEM. On the other, it has evidenced the capability of UVLM to capture the out-of-plane coefficient but its inability to predict in-plane force coefficients due to the absence of viscous drag on an implementation without corrections.

In cases of yaw, the location of the maxima and minima of the blade loads along a revolution at a specific spanwise location is captured by UVLM and LES-AL. In this regard, BEM *no skew* cannot capture the *skewed wake* effect. BEM *skew* provides a too strong correction for this effect estimating the wrong position of the maxima and minima in the root region and too large fluctuations at all spanwise positions. The *advancing/retreating* effect is captured by all the solvers, but in the case of BEM *skew* it is overridden by the previous effect. The location of the maxima and minima locations does not change significantly with the yaw angle and thus these conclusions extend to the whole range of studied yaw angles. This maxima and minima location mismatch is appreciable also in root-bending moments.

The computation of rotor thrust and power coefficients implies integrating along the blade and summing up the three blades. Moreover, the effects of yaw are periodic and thus these coefficients show very small fluctuations. However, these fluctuations increase significantly for yaw angles above $\gamma = 20°$.

In general, all methods predict a consistent decay of coefficients up to an angle of $\gamma = 10°$. After that point the degradation of the coefficients predicted by both BEM methods is significantly larger than for UVLM and LES-AL methods. BEM *skew* predicts the largest fluctuations along a revolution followed by LES-AL and UVLM. On the contrary, BEM *no skew* predicts too small variations.

Acknowledgments

This project has received funding from the European Research Council (ERC) under the European Union's Horizon 2020 research and innovation programme (grant agreement 765579).

References

[1] Pedersen H S and Gil Marín E 2016 Yaw misalignment and power curve analysis URL `http://www.ewea.org/events/workshops/wp-content/uploads/Tech16a-PO-017.pdf`
[2] Gebraad P M O, Teeuwisse F W, van Wingerden J W, Fleming P A, Ruben S D, Marden J R and Pao L Y 2014 *Wind Energy* **19** 95–114
[3] Damiani R, Dana S, Annoni J, Fleming P, Roadman J, van Dam J and Dykes K 2018 *Wind Energy Science* **3** 173–189
[4] Madsen H A, Sørensen N N and Schreck S 2003 Yaw aerodynamics analyzed with three codes in comparison with experiment *41st Aerospace Sciences Meeting and Exhibit* (AIAA)
[5] Hansen M, Sørensen J, Voutsinas S, Sørensen N and Madsen H 2006 *Progress in Aerospace Sciences* **42** 285–330
[6] Burton T, Sharpe D, Jenkins N and Bossanyi E 2001 *Wind Energy Handbook* (Wiley)
[7] Lanzafame R and Messina M 2007 *Renewable Energy* **32** 2291–2305
[8] Rahimi H, Dose B, Stoevesandt B and Peinke J 2016 *Journal of Physics: Conference Series* **749** 012015
[9] 2019 OpenFAST documentation version 1.0 URL `https://openfast.readthedocs.io/en/latest/index.html`
[10] González A and Munduate X 2007 *Journal of Physics: Conference Series* **75** 012020
[11] Katz J and Plotkin A 2001 *Low-Speed Aerodynamics* (Cambridge University Press)
[12] Ramos-García N, Sørensen J N and Shen Z 2018 *Journal of Physics: Conference Series* **524** 012026
[13] Boorsma K, Wenz F, Lindenburg K, Aman M and Kloosterman M 2020 *Wind Energy Science Discussion*
[14] 2019 Github - SHARPy URL `https://github.com/ImperialCollegeLondon/sharpy`
[15] del Carre A, Muñoz-Simón A, Goizueta N and Palacios R 2019 *Journal of Open Source Software* **4** 1885
[16] Murua J, Palacios R and Graham J M R 2012 *Progress in Aerospace Sciences* **55** 46–72
[17] Sørensen J N and Shen W Z 2002 *Journal of Fluids Engineering* **124** 393
[18] Breton S P, Sumner J, Sørensen J N, Hansen K S, Sarmast S and Ivanell S 2017 *Philosophical Transactions of the Royal Society A: Mathematical, Physical and Engineering Sciences* **375** 20160097
[19] Deskos G, Laizet S and Palacios R 2020 *Wind Energy* **23** 779–794
[20] Schepers J *et al.* 2018 *Journal of Physics: Conference Series* **1037** 022013
[21] Sieros G 2017 Redesign of the AVATAR RWT rotor Tech. rep. NTUA
[22] Snel H and Schepers J G 1995 Joint investigation of dynamic inflow effects and implementation of an engineering method Tech. Rep. ECN-C–94-107 ECN